Machine Learning Framework for Time-Resolved Mobility Edges in 1D Quasiperiodic Systems

Shivaji Chaulagain
*Looking For an Affiliation

Abstract

Quasiperiodic systems such as generalized Aubry–André–Harper (AAH) models exhibit rich localization phenomena, including energy-dependent mobility edges that separate extended from localized eigenstates. While machine learning (ML) has recently proven effective in detecting localization transitions in static quasiperiodic and many-body systems, the evolution of mobility edges under time-dependent driving or temporally varying potentials remains largely unexplored. This work proposes a machine learning framework for the time-resolved detection and tracking of mobility edges in quasiperiodic lattices. Focusing on generalized AAH models that support mobility edges, we combine exact diagonalization, wavepacket dynamics, and both supervised and unsupervised ML approaches. Localization indicators such as the inverse participation ratio (IPR), level statistics, and dynamical spreading exponents serve as features and labels to train ML models that can map how mobility edges shift with time or drive parameters. This framework aims to reveal how non-equilibrium driving reshapes the localization landscape, offering new insights into dynamical and Floquet-induced localization in quasiperiodic systems.

1 Introduction

Quasiperiodic systems occupy a fascinating middle ground between crystalline order and complete randomness. They host rich localization behavior that differs fundamentally from conventional Anderson localization [1] in disordered systems. A paradigmatic example is the Aubry–André–Harper (AAH) model, which exhibits a self-dual localization transition at a critical potential strength. However, the standard AAH model features a global transition—either all eigenstates are extended or all are localized—without an energy-dependent mobility edge. In contrast, generalized AAH models incorporating next-nearest-neighbor hopping, asymmetric modulation, or nonlinear onsite potentials can support true mobility edges, where localized and extended states coexist within the same energy spectrum [2–4]. These models have become a fertile ground for studying quantum transport, topological phases, and multifractality in quasiperiodic lattices.

While localization in static quasiperiodic systems is well understood, far less is known about its behavior under time-dependent perturbations. When the potential, phase,

or hopping amplitude evolves dynamically—or under periodic (Floquet) driving—the notion of localization becomes inherently time-resolved. The energy boundary separating localized and extended states, i.e., the mobility edge, may shift or deform as a function of time or drive parameters, giving rise to non-equilibrium localization phenomena that are difficult to capture using traditional analytical tools. Understanding these dynamics is crucial for developing a unified picture of localization in driven quantum systems, with implications for transport control, quantum simulations, and optical lattice experiments [5–7].

Recent advances in machine learning (ML) have demonstrated remarkable capabilities in identifying phase transitions and classifying quantum states directly from raw data [8–10]. In localization studies, ML methods have been successfully applied to detect transition points, predict inverse participation ratios, and uncover hidden features in both single-particle and many-body systems [11–13]. However, most existing works focus on static Hamiltonians, leaving the time-dependent evolution of mobility edges largely unexplored.

In this work, we propose a comprehensive ML-based framework to identify and track time-resolved mobility edges in generalized AAH-type quasiperiodic lattices. By combining exact diagonalization, wavepacket dynamics, and ML techniques—including both supervised classification and unsupervised clustering—we aim to map how localization boundaries evolve with time, drive frequency, and system parameters. The approach leverages localization diagnostics such as inverse participation ratio (IPR), level-spacing ratios, and dynamical spreading exponents as quantitative features for training and validation. Our goal is to develop a robust data-driven methodology for analyzing non-equilibrium localization, providing new insight into how disorder, driving, and quantum interference interact in time-dependent quasiperiodic systems.

2 Model and Theoretical Background

2.1 Generalized Aubry-André-Harper model

We consider a one-dimensional tight-binding Hamiltonian with only nearest-neighbor hopping and a duality-breaking quasiperiodic on-site potential. The Hamiltonian can be written as

$$H = -t_1 \sum_j (c_{j+1}^\dagger c_j + h.c.) + \sum_j V_j c_j^\dagger c_j \tag{1}$$

Here t_1 is the nearest neighbor hopping amplitudes, and the on-site energy at site j is taken to be

$$V_j = \frac{\lambda \cos(2\pi\alpha j + \phi)}{1 - \alpha \cos(2\pi\alpha j + \phi)} \tag{2}$$

In this expression, λ is the modulation strength, α(irrational, e.g. the inverse golden ratio) sets the incommensurate wavevector and ϕ is a tunable phase.

This choice of V_j was introduced by Ganeshan et al. [2] as a controlled deformation of the standard Aubry-André potential. The denominator $1 - \alpha \cos(2\pi\alpha j + \phi)$ effectively adds higher Fourier harmonics and site-dependent shifts that break the self-duality of

the pure cosine model. Physically, the rational form of V_j creates strong varationss (even singular enhancements as $1 - \alpha\cos \to 0$ that cause different energies to localize at different critical strengths. In the limit $\alpha \to 0$ one recovers the usual sinusoidal Aubry-André model, which has the well-known property that all states localize simultaneoulsy at a single critical λ/t_1 (i.e. no mobility edge) [2]. By contrast, for $\alpha \neq 0$ the duality symmetry is broken: extended and localized states can coexist. Ganeshan et al. proved that this nearest-neighbor model is self-dual under a generalized transformation, and they derived an exact analytic mobility edge $E_c(\lambda, \alpha)$ separating localized and extended states [2] .

2.2 Quasiperiodic lattice and localization

Since α is irrational, V_j is quasiperiodic (deterministically "pseudorandom"). Quasiperiodicity leads to localization via destructive interference, much like Anderson Localization but without true disorder [2]. In the standard Aubry-André model ($\alpha = 0$), this yields a sharp transition at $\lambda/t_1 = 2$ where all single-particle states switch from extended ($\lambda < 2$ to localized ($\lambda > 2$) [2]. Crucially, that transition is energy-independent: there is no mobility edge in the pure sinusoidal model [2].

By contrast, the deformed potential above generically produces an energy-dependent (single-particle) mobility edge. Ganeshan et al. showed that the self-duality condition in this model can be written in closed form as a function of energy, yielding a critical line $E_c(\lambda, \alpha)$ [2]. Numerical diagnostics (such as the inverse participation ratio and the typical density of states) indeed reveal that for $\lambda > 0$, states with $|E| < |E_c|$ remain extended while those with $|E| > |E_c|$ become localized [2]. In other words, there is a mixed "intermediate phase" where localized and extended eigenstates coexist, bounded by the mobility edge.

This behavior is consistent with other theoretical studies of 1D quasiperiodic models. For example, Xiao Li and Das Sarma demonstrated that realistic bichromatic optical lattices always exhibit mobility edges unless one is in the extreme tight-binding limit [3]. In their words, the pure Aubry–André description "generically breaks down" near the transition because "single-particle mobility edges (SPME)" unavoidably appear [3]. Our rational potential can be viewed as embodying those additional Fourier components: the denominator $1 - \alpha\cos(...)$ introduces precisely the kind of harmonic content that Li et al. identify as causing the mobility edge [3].

2.3 Time-dependent driving and modulation

We introduce explicit time dependence into the Hamiltonian by allowing parameters such as the potential strength V or phase ϕ to vary in time: $V \to V(t)$ and/or $\phi \to \phi(t)$. Two cases are of interest. Periodic (Floquet) driving: $V(t) = V_0 + V_1\cos(\omega t)$ or $\phi(t) = \phi_0 + \Omega t$ with period $T = 2\pi/\omega$. In this scenario $H(t + T) = H(t)$ one can analyze the system using Floquet theory. The stroboscopic evolution over one period is governed by an effective Floquet Hamiltonian H_F (via $U_F = e^{-iH_F T}$), whose quasi-energy spectrum can show new localization features. For instance, recent work found that periodic modulation of the Aubry–André potential can induce a mobility edge that

is absent in the static model [14]. Specifically, a Floquet mobility edge appears separating localized and delocalized Floquet eigenstates, even though the undriven AAH model had none [14]. This edge influences long-time transport (e.g. survival probability and Shannon entropy of a particle) in distinct ways.

By contrast, slow non-periodic modulation means parameters vary in time without fixed periodicity (e.g. a linear ramp $V(t) = V_0 + \alpha t$ or a random slow variation of phase). In this case the spectrum evolves continuously, and we can track the instantaneous localization transition as the system is quenched or ramped. Both types of driving allow one to probe "time-resolved" mobility edges: energy thresholds that change with t as $V(t)$ or $\phi(t)$ evolve. Conceptually, the evolving Hamiltonian $H(t)$ leads to a time-dependent Schrödinger equation

$$i\frac{d}{dt}|\psi(t)>= H(t)|\psi(t)>, \tag{3}$$

and one monitors how localization properties change in real time. In the Floquet case $|\psi(t+T)\rangle = U_F|\psi(t)\rangle$, while in the slow-drive case one may use adiabatic approximations or numerical integration. In either case, the Hamiltonian (1) with its tunable parameters provides a natural testbed for machine-learning schemes that aim to detect mobility edges as functions of time.

2.4 Dynamical and spectral diagnostics

2.4.1 Wavepacket dynamics

We consider an initially localized state ($|\psi(0)\rangle = c_{j_0}^\dagger|0\rangle$ at site j_0) and compute its time evolution under $H(t)$. In the site basis the wavefunction amplitudes $\psi_j(t) = \langle j|\psi(t)\rangle$ satisfy

$$i\frac{d}{dt}\psi_j(t) = -t_1[\psi_{j+1}(t) + \psi_{j-1}(t)] + V_j(t)\psi_j(t) \tag{4}$$

which follows directly from Eq.(1). We then compute moments of the wavepacket - the mean-square displacement - as

$$\sigma^2(t) = \sum_j (j - j_0)^2|\psi_j(t)|^2, \tag{5}$$

as well as the survival probability $P_{j_0}(t) = |\psi_{j_0}(t)|^2$. In an extended regime the packet will spread and $\sigma^2(t)$ grows (often ballistically or diffusively), whereas in a localized regime $\sigma^2(t)$ saturates. These dynamical signatures, including long-time $P_{j_0}(t)$, serve as indicators of localized vs. extended behavior during the drive.

2.4.2 Inverse Participation Ratio (IPR)

For each (Floquet or instantaneous) eigenstate $|\phi_n\rangle$ we compute

$$IPR_n = \sum_j |<j|\phi_n>|^4, \tag{6}$$

which measures localization of that state. Here IPR $\sim O(1)$ for a fully localized state and IPR $\sim 1/N$ for a state extended over N sites. As shown in [46†L99-L102], one

can plot IPR_n versus eigenenergy to locate the mobility edge: states on one side of the edge have high IPR (localized) and on the other side low IPR (extended) [2]. We also monitor the typical density of states or the averaged IPR across energy windows as an order parameter for localization.

2.4.3 Level spacing statistics (r-statistic)

We compute the eigenvalues E_n of $H(t)$ (or the quasi-energies of H_F) and form the spacings $s_n = E_{n+1} - E_n$. The ratio

$$r_n = \frac{min(s_n, s_{n-1})}{max(s_n, s_{n-1})} \tag{7}$$

provides a normalized measure of spectral rigidity. In practice one evaluates the average $\langle r \rangle$ over all n. A value $\langle r \rangle \approx 0.53$ indicates extended (Wigner–Dyson) level correlations, whereas $\langle r \rangle \approx 0.39$ signals uncorrelated (Poisson) statistics characteristic of localized states. Thus $\langle r \rangle$ jumps across a mobility edge as one moves in energy. Tracking $\langle r \rangle$ as a function of energy (or time) offers an additional way to detect the transition point between localized and extended spectral regimes.

3 Computational Methods

The computational study was carried out using `Python` with the `NumPy` and `SciPy` libraries for linear algebra and sparse-matrix operations. Both open and periodic boundary conditions were considered to capture edge effects and ensure that localization properties are not artifacts of finite-size geometry. The lattice size ranged from $L = 200$ to 1000 sites, large enough to achieve smooth spectral statistics while remaining computationally feasible for repeated diagonalization and time evolution.

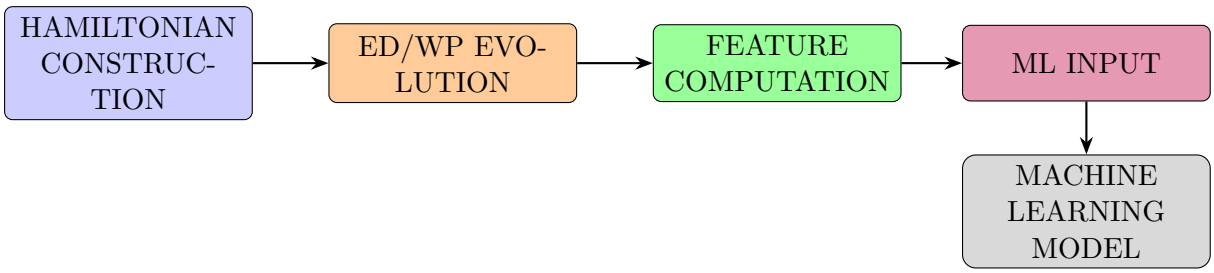

Figure 1: Flowchart of the Computational Pipeline

For each set of parameters, the generalized Aubry–André–Harper Hamiltonian matrix was constructed as a sparse Hermitian operator. The matrix is tridiagonal for the standard AAH case and becomes pentadiagonal when next-nearest-neighbor hopping is included. Because the matrix contains only $O(L)$ nonzero elements, it was stored in compressed sparse format to optimize both memory and performance. The exact diagonalization of the static or instantaneous Hamiltonian was performed using the `SciPy` ARPACK eigensolver for large systems or the dense routine for smaller systems. The

ARPACK method was particularly useful when only a subset of eigenvalues and eigenvectors—typically those near the center of the spectrum—were needed for calculating localization measures with high energy resolution.

From each diagonalization step, the eigenvalues and eigenvectors were used to compute localization observables. The inverse participation ratio was obtained from the normalized eigenstates, allowing energy-resolved identification of localized and extended regions. The level-spacing ratio (r-statistic) was calculated from consecutive energy spacings to characterize spectral correlations. The average ratio $\langle r \rangle > \approx 0.53$ indicates delocalized (Wigner–Dyson) statistics, while $\langle r \rangle \approx 0.39$ signals localized (Poisson) behavior, providing an independent verification of the IPR-based results.

For studying real-time dynamics, the time-dependent Schrödinger equation was integrated numerically using the Crank–Nicolson scheme, a second-order implicit method that conserves the wavefunction norm and ensures numerical stability even for long simulation times. This scheme solves a linear system at each timestep, which was efficiently handled using sparse LU decomposition in `SciPy`. The time step Δt was chosen between 0.005 and 0.01 (in units of $\hbar/J$) based on convergence tests, and the total simulation time typically ranged from $t = 0$ to 1000. For periodically driven systems, the time-dependent Hamiltonian was updated at each step according to the modulation protocol (e.g., varying potential amplitude or phase).

To balance accuracy and storage, observables were sampled less frequently than the integration timestep. The Hamiltonian snapshots were saved every few drive cycles or after fixed time intervals, while wavefunction observables—such as site probabilities $|\psi(t)|^2$, mean-square displacement $\sigma^2(t)$, and survival probability $P(t)$—were recorded every 10–50 timesteps. For long runs, logarithmic sampling was adopted to capture both short- and long-time dynamics without excessive data size. Rather than storing full wavefunctions, only summary observables and moments were kept, which significantly reduced storage needs while retaining the physical information necessary for analysis.

The computed data were used to generate a set of machine learning features. From the diagonalization results, energy-resolved IPR and level-spacing ratios formed the static features, while from the dynamical simulations, quantities such as $\sigma^2(t)$, its time-dependent power-law exponent γ (where $\sigma^2(t) \propto t^\gamma$, and the return probability $P(t)$served as time-resolved descriptors. Together, these observables capture both spectral and dynamical aspects of localization and delocalization. Before feeding them to the learning model, all features were normalized, and selected data were averaged over several random phase offsets of the quasiperiodic potential to improve statistical reliability.

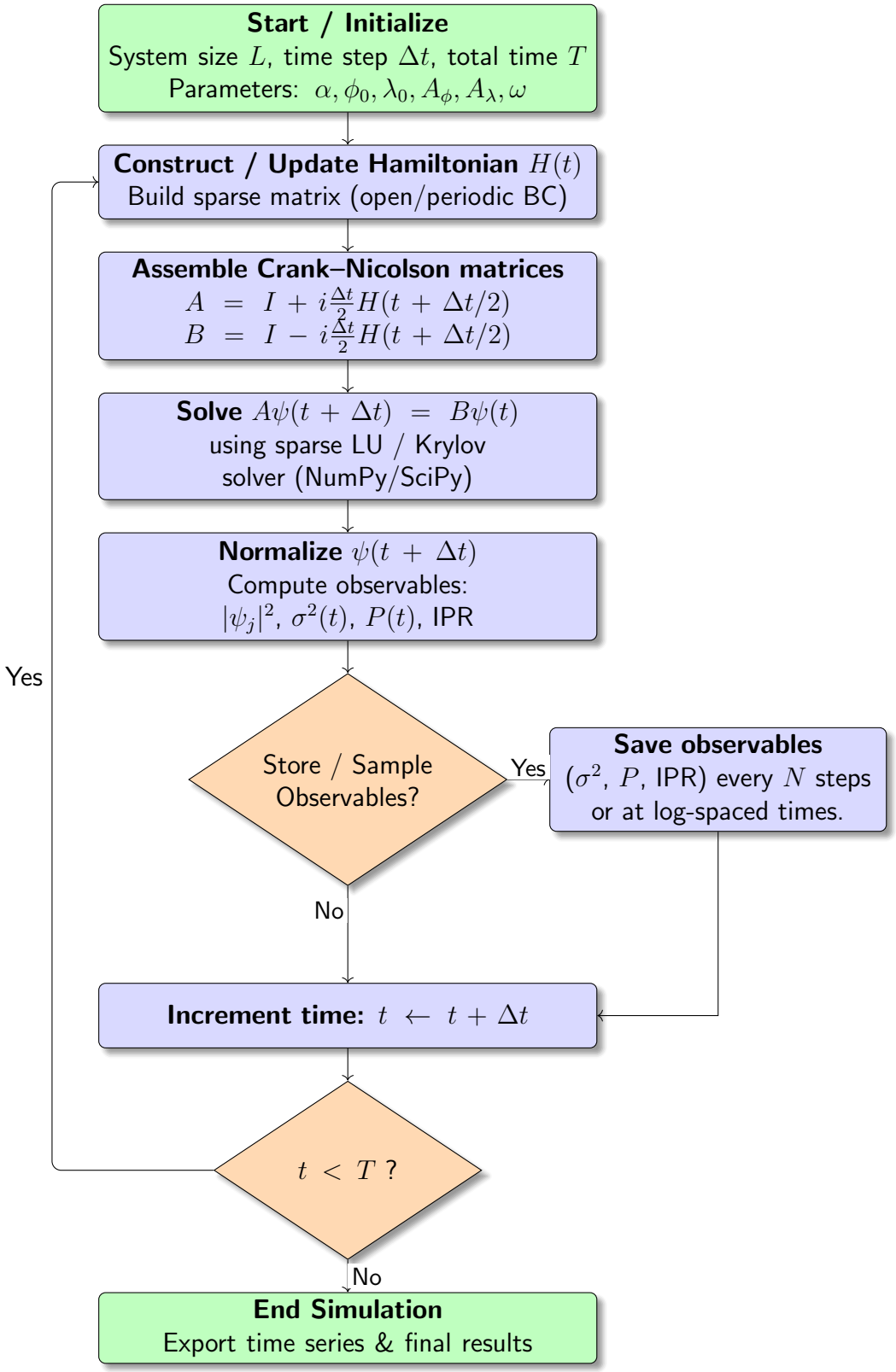

Figure 2: Flowchart of the Crank–Nicolson Time-Stepping Algorithm for the Driven Quasiperiodic System.

References

[1] P. W. Anderson. Absence of diffusion in certain random lattices. *Phys. Rev.*, 109:1492–1505, Mar 1958.

[2] Sriram Ganeshan, Jed H. Pixley, and S. Das Sarma. Nearest neighbor tight binding models with an exact mobility edge in one dimension. *Physical Review Letters*, 114(14):146601, 2015.

[3] Xiaopeng Li and S. Das Sarma. Mobility edges in one-dimensional bichromatic incommensurate potentials. *Physical Review B*, 96(8):085119, 2017.

[4] Michele Modugno. Exponential localization in one-dimensional quasi-periodic optical lattices. *New Journal of Physics*, 11(3):033023, 2009.

[5] David J. Luitz and Yevgeny Bar Lev. Many-body localization edge in the random-field heisenberg chain. *Annalen der Physik*, 529(7):1600350, 2017.

[6] C. Dai, Y. Zhang, and J. Zhang. Floquet engineering of mobility edges in one-dimensional quasiperiodic lattices. *Physical Review B*, 103(1):014205, 2021.

[7] Norman Y. Yao and Andrew C. Potter. Floquet localization and time crystals in driven quasiperiodic systems. *Annual Review of Condensed Matter Physics*, 10:233–252, 2019.

[8] Juan Carrasquilla and Roger G. Melko. Machine learning phases of matter. *Nature Physics*, 13(5):431–434, 2017.

[9] Evert P. L. Van Nieuwenburg, Ye-Hua Liu, and Sebastian D. Huber. Learning phase transitions by confusion. *Nature Physics*, 13(5):435–439, 2017.

[10] Eliska Greplová and Evert P. L. van Nieuwenburg. Unsupervised identification of topological phase transitions using predictive models. *Nature Machine Intelligence*, 2(9):542–549, 2020.

[11] Jordan Venderley, Vedika Khemani, and Eun-Ah Kim. Machine learning out-of-equilibrium phases of matter. *Physical Review Letters*, 120(25):257204, 2018.

[12] Frank Schindler, Nicolas Regnault, and Titus Neupert. Many-body localization transition with symmetry-protected topological states. *Physical Review B*, 95(24):245134, 2017.

[13] Ren Yu, Xiaodong Gao, and Shun-Qing Shen. Identifying quantum phase transitions with unsupervised learning. *Physical Review B*, 102(8):085116, 2020.

[14] Madhumita Sarkar, Roopayan Ghosh, Arnab Sen, and K. Sengupta. Mobility edge and multifractality in a periodically driven aubry-andré model. *Physical Review B*, 103(18), May 2021.